

Final Draft
of the original manuscript:

Bohlen, J.; Wendt, J.; Nienaber, M.; Kainer, K.U.; Stutz, L.; Letzig, D.:
**Calcium and zirconium as texture modifiers during rolling
and annealing of magnesium–zinc alloys**
In: Materials Characterization (2015) Elsevier

DOI: [10.1016/j.matchar.2015.02.002](https://doi.org/10.1016/j.matchar.2015.02.002)

Calcium and zirconium as texture modifiers during rolling and annealing of magnesium-zinc alloys

Jan Bohlen*, Joachim Wendt, Maria Nienaber, Karl Ulrich Kainer, Lennart Stutz, Dietmar Letzig

Magnesium Innovation Centre, Helmholtz-Zentrum Geesthacht, Max-Planck Str. 1, 21502 Geesthacht, Germany

*corresponding author: jan.bohlen@hzg.de; phone: +49-4152-87-1995

Abstract

Rolling experiments were carried out on a ternary Mg-Zn-Ca alloy and its modification with zirconium. Short time annealing of as-rolled sheets is used to reveal the microstructure and texture development. The texture of the as-rolled sheets can be characterised by basal pole figures with split peak towards the rolling direction (RD) and a broad transverse angular spread of basal planes towards the transverse direction (TD). During annealing the RD split peaks as well as orientations in the sheet plane vanish whereas the distribution of orientations tilted towards the TD remains. It is shown in EBSD measurements that during rolling bands of twin containing structures form. During subsequent annealing basal orientations close to the sheet plane vanish based on a grain nucleation and growth mechanism of recrystallisation. Orientations with tilt towards the TD remain in grains that do not undergo such a mechanism. The addition of Zr delays texture weakening.

Keywords: magnesium alloys, sheet rolling, microstructure, texture, recrystallization, X-ray diffraction, Electron backscattering diffraction (EBSD)

Introduction

Conventional magnesium sheets, like those known from magnesium alloy AZ31, lack in enhanced formability, especially at room temperature. Numerous works have shown that a texture variation can help to overcome this issue [1, 2, 3, 4, 5]. The typical strong alignment of basal planes in conventional magnesium sheets limits the strain accommodation during deformation as well as the resulting work hardening ability [6]. If textures are weaker, higher ductility even at room temperature as well as improved formability can be achieved.

It has been shown that adding rare earth elements results in texture weakening characterised by a tilt of basal planes away from the sheet plane. Several approaches have been used to explain this behaviour which is very different compared to the same alloys without addition of rare earth elements [7]. The mechanisms which are considered to lead to such texture changes draw a line from changes in the active deformation mechanisms, such as slip modes [6, 8, 9, 10, 11], different types of twins [7, 12] and shear bands [13, 14] to changes during microstructure reformation as a result of recrystallisation [13, 15, 16, 17, 18].

In an attempt to overcome the necessity of including rare earth elements to improve sheet properties, actual works deal with alternative approaches, e.g. considering calcium (Ca) as an alloying element in magnesium. This can result in very similar effects in the texture development during rolling, e.g. [19]. Again, texture effects are those that significantly contribute to improved formability of such sheets.

Ca as an alloying element in magnesium has some features that compare well to those of rare earth elements, such as a size misfit in the magnesium lattice structure or a decrease of stacking fault energies [20, 21]. Corresponding to this, it was found that Ca additions to Mg-Zn alloys lead to textures that have strong similarities with those of rare earth elements containing Mg-Zn sheets [5, 22]. In these works a strong contribution of different twin types and subsequent static recrystallisation are emphasised as texture determining mechanisms.

In this work a Mg- 1 wt.% Zn-0.5wt.% Ca with and without Zr as a grain refiner in magnesium alloys is used and the developing microstructure during rolling is investigated. The sheets were analysed before and during annealing in order to track the texture development and reveal the significance of different mechanisms on the microstructure formation.

Experimental

Gravity die-cast billets of two alloys, ZX10 (Mg + 0.91 wt% Zn + 0.52 wt% Ca) and the zirconium containing modification ZXK100 (Mg + 0.86 wt% Zn + 0.51 wt% Ca + 0.08 wt.% Zr) were used to cut slabs (dimensions: 20 mm thickness, 280 mm width and 50 mm length) for rolling experiments. A solution annealing was carried out for 16 hours at 450°C prior to rolling. A 50 ton laboratory rolling stand with cold rolls of 400 mm diameter was used to carry out rolling experiments on both alloys at 400°C. A rolling procedure with increasing degree of deformation per pass was applied, starting with 4 passes of 0.1 followed by 7 passes of 0.2 and 3 passes of 0.3. The same rolling schedule has been applied in earlier work [12].

In case of ZXK100 two passes of 0.05 were applied instead of the first pass with 0.1 to avoid early cracking of the sample. The rolling speed was constant at 16 rounds per minute. Between the passes the samples were reheated to 400°C for 15 min. The as-rolled sheets were used to apply annealing experiments at 400°C for various times in order to track the microstructure development. For this purpose the samples were put into a circulating air furnace for very short periods of 15 s, 30 s, 45 s, 60 s, 90 s and 300 s. Obviously, the sample did not reach the targeted temperature at these short annealing times but the procedure is consistent with a technical annealing process. Furthermore, one sample was annealed for 1800 s (30 min). All samples were air-cooled after annealing.

Standard metallographic sample preparation procedures were applied and an etchant based on picric acid was used [23] to reveal the microstructure in optical microscopy. Texture measurements were performed on samples ground and polished to their mid-planes. A Panalytical X-ray diffractometer with Cu K α radiation was used to measure six pole figures up to a sample tilt of 70°. A computer code MTEX [24] was applied to calculate the orientation distribution function and recalculate full pole figures. Electron backscatter diffraction (EBSD) was used to measure local orientation patterns on a field emission gun scanning microscope (Zeiss, Ultra 55, EDAX/TSL) from longitudinal sections of the samples. Measurements were repeated at different sections of the samples to verify the reproducibility of results. An accelerating voltage of 15 kV and a step size of 0.3 μm were used. Sample surfaces were prepared in the same way as for metallography and were then electropolished using an AC2 solution (StruersTM). A software “TSL Orientation Imaging Microscopy Analysis” of EDAX[©] was employed to analyse the EBSD measurements. Different data cleaning procedures were tested using TSL cleanup functions. A cleanup procedure consisting of a grain confidence index (CI) standardisation and a neighbour CI correlation was applied. The first function allows measured points with low CI but similar orientation like the surrounding measured points to be rated as properly indexed. A grain tolerance angle of 5° and a minimum grain size of 2 points were selected. The second function is applied on measured points with a CI lower than 0.04. In case of a point with lower CI the neighbour with the highest confidence index is selected and the orientation is replaced. The combination of both cleanup functions allows a clear identification of boundaries. There has been no significant impact on the resulting textures of this work especially in comparison to other data processing approaches including a simple CI selection of points with different point CI, e.g. 0.03 or 0.05. EBSD data analysis especially included a function to separate grains with different grain orientation spread (GOS). An additional limitation of a minimum grain size of 0.6 μm (again 2 measured points) was set. In this approach an average orientation is

determined for a respective grain. The deviation for each measured point in this grain from the average orientation is then calculated and averaged as the GOS. The software then allows separation of grains with specified GOS.

Results

Fig. 1 collects micrographs after rolling as well as after annealing of the ZX10 (Fig. 1a) and ZXK100 (Fig. 1b) sheets. For both alloys significant changes in the microstructure are found even as a result of short-time annealing. In the as-rolled condition a deformed microstructure of originally equiaxed grains contains a high concentration of twins. The main difference in the grain structure of the two sheets is the grain size which is finer in case of ZXK100 than in the case of ZX10. When annealing starts, e.g. after 15 s, the microstructures change and exhibit bands of dark lines across the grains. Only with increasing annealing time (30 s) it becomes visible that these bands stem from small grains which grow into the deformed microstructure. They develop into a partly recrystallised microstructure after 45 s annealing. After 60 s annealing an almost recrystallised microstructure is observed with an average grain size of 6 μm for alloy ZX10 and 5 μm for alloy ZXK100 which is a distinctly finer grained microstructure for both alloys than in their as-rolled condition. Subsequent grain growth up to the longest annealing time of 1800 s then reveals microstructures with grain sizes comparable to the as-rolled conditions. ZXK100 is finer grained (8 μm) compared to ZX10 (15 μm). Fig. 1c shows the development of the average grain size of the recrystallised microstructures up to this highest annealing time. It can be seen that the grain size of ZX10 is larger than of ZXK100 and the tendency to grain growth is more distinct in ZX10 than in ZXK100.

Fig. 2 shows pole figures of basal planes (0002) and prismatic planes (10-10) to reveal the texture of the as-rolled and annealed sheets. The texture of the two alloy sheets is comparable in the as-rolled condition, i.e. the basal pole figures show a split peak to the rolling directions

(RD), low intensities in the normal direction (ND) and a broad angular distribution of basal planes towards the transverse direction (TD). The peak intensities are slightly higher for ZXK100 than for ZX10. With increasing annealing time the significance of the RD split peaks decreases until they vanish after 60 s. After this point a further decrease of the intensities leads to the visualisation of split peaks with low intensity and a tilt towards the TD, named a TD split. However, the intensities of this texture component are not very distinct and especially not very different if compared to the intensities at the same orientations at lower annealing times. Furthermore, this component does not newly develop as a result of annealing, but it appears to be a remainder of an ongoing decrease of intensities in the ND as well as in the RD split peak orientations. For ZXK100 the vanishing of such orientations required higher annealing times compared to ZX10. It is noted, that the changes in the prismatic pole figure are small, exhibiting a preferential alignment of prismatic planes parallel to the rolling direction. A slight preference with higher intensity in the RD may be revealed.

The above described texture development is concurrent to the formation of new grains during recrystallisation that grow into the as-rolled microstructure during annealing. In order to reveal different grain fractions and their orientation development during annealing, EBSD orientation patterns are used. Results for the as-rolled condition are shown in Fig. 3 for both alloys as boundary maps. Numerous boundaries can be identified as grain boundaries (black) or can be associated with low angle grain boundaries (grey). Furthermore, different types of twin boundaries can be revealed in both alloys, i.e. $\{10-12\}$ -“tensile” twins (red), $\{10-11\}$ -“compression” twins (blue) and $\{10-11\}/\{10-12\}$ “double” twins (yellow). This allows the separation of twinned areas of the microstructure for an orientation analysis. Specifically, the orientations of double twins correspond well with the RD split peaks. A similar finding has also been shown in an early work by Couling et al. [25]. Tensile twins are oriented off the ND which also includes TD split orientations. Furthermore, entirely other orientations are also

found. The same also holds for compression twins. The principal finding is comparable for the two alloys but the area fraction of twins is 2 – 3 times higher in ZX10 than in Z XK100.

In Fig. 4 orientation patterns of the sheets are shown in the as-rolled condition and after annealing for 15 s and 30 s, respectively (Fig. 4a-c for ZX10 and Fig. 4d-f for Z XK100). The complete microstructure is shown in the first line labelled “all grains”. It shows a microstructure development consistent with the findings in Fig. 1. During annealing small grains develop throughout the microstructure, partly in bands that consist of twins in correspondence to Fig. 3.

The microstructures are then separated into fractions by using the grain orientation spread (GOS) as a separator. In doing this, it is assumed that small grains with low orientation spread are the result of a grain nucleation and growth mechanisms during recrystallisation [26]. The specific limit of 1° is arbitrarily chosen in an attempt to reveal only such small grains from the full microstructure. Results are shown in the line labelled “GOS < 1° ”. In the as-rolled conditions of both alloys in Figs. 4a and 4d the above mentioned band-like structures of small grains are revealed. Interestingly, in Z XK100 these structures of new grains appear to be more developed than in ZX10. The texture of these fractions of the microstructure is weak and mainly of a basal type (specifically in Fig. 4a), i.e. basal planes are aligned parallel to the sheet plane. Some intensity is also found in other orientations like in Fig. 4d which can be associated with twins that also appear as regions with low GOS. Vice versa, a fraction of grains with GOS larger than 3° is separated in order to reveal orientation of grains that underwent deformation but did not recrystallise after the final rolling pass. This line is labelled “GOS > 3° ”. The texture consists of tilted peaks to the RD as well as to the TD rather than of orientations in ND. Note, that twins are mostly excluded from this fraction as a result of the chosen constraint. After 15 s annealing in Figs. 4b and 4e the finding is similar in this fraction of grains with high GOS. However, recrystallised grains with GOS < 1° reveal a

further developed band-like structure. The texture of this fraction is weak for ZX10 without specific alignment of grains whereas for ZXK100 a weak basal texture is revealed. It is noteworthy, that both alloys do not show orientations with TD split orientations in this fraction of recrystallised grains.

Unlike this, after 30 s annealing in Figs. 4c and 4f orientations with TD tilt occur in the recrystallised fraction of the microstructure ($GOS < 1^\circ$) of both alloys. The recrystallised grain size is significantly larger for both alloys compared to the ones after lower annealing time and it is not possible any more to reveal the above mentioned deformation bands. The unrecrystallised fraction of the microstructure with $GOS > 3^\circ$ still reveals split peaks to RD as well as to TD. It is noted that for both alloys 30% of the microstructure remain unrecrystallised with high GOS.

The last line of Figs. 4 a-f, labelled “TD orientations highlighted” shows highlighted grains with TD split orientations. Grains with this orientation are also visible in the band-like structures of newly nucleated grains. However, for both alloys mainly grains which did not undergo recrystallisation after the final rolling pass exhibit this orientation. Furthermore, it is found that different grains are sectioned by small angle grain boundaries. However, an orientation specific preference of such sectioning cannot be revealed.

In summary of Fig 4 new grains develop during annealing as a result of a grain nucleation and nucleation growth mechanism in zones of deformation bands or twin bands. These zones are associated with textures of random character or those that are of a weak basal type. It cannot be revealed from these measurements if there is a preferential growth of such grains during annealing. Grains that do not undergo recrystallisation in terms of grain nucleation and grow maintain orientations with TD split.

Fig. 5 collects data of different fractions of grains revealed from the EBSD measurements shown in Fig. 4 in order to quantify the relative amount of grains with RD tilt or TD tilt orientations. As expected, the overall fraction of recrystallised grains with $GOS < 1^\circ$ increases with annealing time for both alloys whereas the fraction of unrecrystallised grains with $GOS > 3^\circ$ decreases with annealing time. As part of these respective total fractions of recrystallised or unrecrystallised grains the relative part of grains with RD tilt orientation or TD tilt orientation is compared. Grains with RD tilt are selected by looking at those grains with a tilt of 45° towards RD and an angular deviation of this orientation of up to 30° . Grains with TD tilt are selected in the same way but with a tilt of 45° into TD. Fig. 5a includes a legend to identify the selected orientations with RD tilt or TD tilt. In case of ZX10 the fraction of recrystallised grains with $GOS > 1^\circ$ and RD tilt increases with the annealing time. However, relatively it remains unchanged making ca. 25% of the recrystallised grains in all three annealing conditions. In case of ZXK100 the finding is similar with ca. 30% of the recrystallised grains. In case of grains with TD tilt orientation there is a relative increase as part of the overall fraction of recrystallised grains, increasing from 25% to 49% in case of ZX10 and from 29% to 41% in case of ZXK100 during annealing. As a result a tendency to develop grains with TD tilt orientations in relation to the overall orientation distribution can be verified. Contrary, the relative fraction of unrecrystallised grains ($GOS > 3^\circ$) with RD or TD tilt remains almost unchanged during annealing, being ca. 30% for RD tilt grains and ca. 50% for TD tilt grains. Thus, a preferential orientation which forms recrystallised grains cannot be revealed from the unrecrystallised fraction of the microstructure.

Discussion

Attempts have been made to correlate the development of specific texture components in magnesium sheets to specific deformation mechanisms and preferential orientation growth during recrystallisation.

E.g. higher activity of prismatic slip has been correlated with the development of a TD spread of basal planes [8] or of $\langle c+a \rangle$ pyramidal slip with the development of RD split peaks [9]. Generally, it has also been shown in earlier work [27] that ambient temperature tensile tests along any direction of a sheet will form textures with a spread of basal planes transverse to the testing direction. A similar behaviour can thus be proposed for applying a rolling pass. The respective texture development is then understood as a result of reorientations because of activated deformation mechanisms. Orientations in the unrecrystallised fractions of the microstructures of this study are also assumed to be related to such mechanisms, which is supported by the textures of the fractions of grains with high GOS in Fig. 4 ($\text{GOS} > 3^\circ$).

Specifically, the importance of twins is often stressed in the context of texture development [12, 16]. Different types of twins have been associated with the formation of a TD component. In [28] the formation of tensile twins is associated with the above mentioned spread of basal planes perpendicular to a tensile testing direction. In [5] tensile twins are seen as a source for TD split orientations in Ca containing alloys with higher Zn content during rolling. Although these considerations also correspond to twin orientations revealed in Fig. 3, the alloys of this study also exhibit large unrecrystallised grains as the distinct source of TD orientations rather than twins.

To a large extent twins are conglomerated in band-like structures, a term used in order to avoid the term “shear bands”. In this it has to be given respect to the fact that different types of such bands may have different origin. In Ion et al [16] shear bands are seen as a result of dynamic recrystallisation based on local rotations of subgrains formed at grain boundaries which lead to a different orientation development compared to the same considerations at twin boundaries. Nie et al. [29] reveal a mechanism of twin boundary stabilisation as a result of element segregation, specifically of rare earth elements, to twin boundaries. It is hypothesised that Ca as an alloying element has a similar effect. In such a case, twins more likely play a role in subsequent recrystallisation based on the high stored energies in such regions. In Fig. 4

it is confirmed that static recrystallisation occurs in a grain nucleation and growth mechanism along these highly twinned fractions of the microstructure. This respective fraction of grains then contributes to an overall texture randomisation. Interestingly, the texture weakening during annealing of ZXK100 appears to be delayed with respect to such a mechanism. On the other hand, the recrystallised grain structure is slightly finer grained in ZXK100 than in ZX10. In a later stage of annealing, see Fig. 1, a growth limitation of grains is found in the Zr containing alloy ZXK100, resulting in a finer grained microstructure after annealing.

One consideration then is that such a resulting finer grained microstructure after annealing is also representative for the condition prior to an upcoming rolling pass, i.e. the annealed condition can be seen as representative for the sheet before the final (or even an earlier) rolling pass. The resulting difference in the grain structure will also develop during the rolling process, i.e. during annealing between two rolling passes. In this case a finer-grained alloy ZXK100 compared to ZX10 receives the respective deformation and again, the discussed mechanisms of deformation, including twinning, accommodate strain. Then, it is suggested to consider an effect of the grain size of the sheet on the twinning activity during the rolling pass. It has been shown that there is a grain size dependence on the activation and growth of twins which is limited if the grains are smaller [30, 31, 32]. If twins are less significant in their appearance and thus have a limited effect during recrystallisation as revealed above, a less significant weakening of the respective texture component can be the result. Furthermore, a grain boundary formation of grains and corresponding band structures (i.e. bands not originating from twins) will not lead to significant changes in the texture [16, 33].

Grains with TD orientations are principally those that did not undergo recrystallisation based on a nucleation and growth mechanisms. However, mechanisms like recovery or continuous grain formation can explain that such grains appear with low GOS. Interestingly, RD split

orientations are consumed during recrystallisation whereas TD split orientations are not, although both types of grains are revealed as unrecrystallised large grains with high GOS.

Vice versa, if the annealed condition of the sheets again is considered as the origin for an upcoming rolling pass, the as-rolled condition can be seen as the result of the applied deformation. Again, no distinct intensity changes of TD-orientations are found but orientations with RD split orientations or those aligning basal planes close to the sheet plane develop which are those that vanish again during annealing.

In the subsequent development of the microstructure after longer annealing a growth limitation of the primary recrystallised microstructure is revealed in ZXK100 compared to ZX10. This finding can be directly correlated to the addition of Zr. As a result, the texture development after annealing is comparable for the two alloys of this study, leaving the ZXK100-sheet distinctly finer grained compared to the ZX10-sheet. In [6] a similar result is derived for a Zr modified ZE10-sheet, also revealing no specific effect on the texture.

Summary and Conclusion

Ca as an alloying element in magnesium-zinc contributes to a similar texture development during rolling and annealing like rare earth elements do. A mechanism of grain nucleation and growth explains a texture randomisation effect in band-like structures consisting of twins. The twinned fraction of the microstructure is found as a source of randomly oriented grains. Furthermore, grains with TD orientations do not preferentially undergo such a grain nucleation and growth mechanism but are likely the result of recovery or an arrangement of subgrains to form high angle grain boundaries. The addition of Zr delays the texture development, hypothetically by influencing the fraction of twinned microstructure due to the smaller grain size. During subsequent annealing the differences in the textures of the alloys

vanish whereas a grain growth limitation can be ascribed to the addition of Zr. It is hypothesised that the impact of mechanisms such as a random textured grain nucleation and growth or a recovery mechanism of TD tilt grains become distinct in the alloys of this study (or in other rare earth containing magnesium alloys) because of a significant growth restriction of grains with alignment of the c-axis close to the ND as typically observed in classical wrought alloy sheets like from AZ31.

Acknowledgements

The authors appreciate help of Mr. Günter Meister and Mr. Alexander Reichart during material preparation and the help of Mrs. Petra Fischer during EBSD experiments.

References

- [1] H. Friedrich, S. Schumann, *J. Mater. Process. Tech.* 117 (2001) 276 – 281.
- [2] Y. Chino, K. Sassa, M. Mabuchi, *Mater. Sci. Eng. A* 513-514 (2009) 394–400.
- [3] C.E. Dreyer, W.V. Chiu, R.H. Wagoner, S.R. Agnew, *J. Mat Proc. Techn.* 210 (2010) 37 – 47.
- [4] L. Stutz, J. Bohlen, G. Kurz, D. Letzig, K.U. Kainer, *Key Eng. Mater.* 473 (2011) 335 – 342.
- [5] J.Y. Lee, Y.S. Yun, B.C. Sue, N.J. Kim, W.T. Kim, D.H. Kim, *J. Alloys Compd.* 589 (2014) 240-246.
- [6] J. Bohlen, M.R. Nürnberg, J.W. Senn, D. Letzig, S.R. Agnew, *Acta Mater.* 55 (2007) 2101–2112.
- [7] L.W.F. Mackenzie, M.O. Pekguleryuz, *Scripta Mater.* 59 (2008) 665-668.
- [8] A. Styczynski, C. Hartig, J. Bohlen, D. Letzig, *Scripta Mater.* 50 (2004) 943-947.
- [9] S.R. Agnew, M.H. Yoo, C.N. Tomé, *Acta Mater.* 49 (2001) 4277-4289.

- [10] J.P. Hadorn, K. Hantzsche, S. Yi, J. Bohlen, D. Letzig, J.A. Wollmershauser, S.R. Agnew, *Metall. Mater. Trans. A* 43 (2012) 1347 – 1362.
- [11] S. Sandlöbes, S. Zaeferrer, I. Schestakow, S. Yi, R. Gonzalez-Martinez, *Acta Mater.* 59 (2011) 429 – 439.
- [12] K. Hantzsche, J. Wendt, K.U. Kainer, J. Bohlen, D. Letzig, *JOM* 61 (8) (2009) 38–42.
- [13] J.W. Senn, S.R. Agnew, *Proc. Magnesium Technology in the Global Age*, Montreal, Canada, (2006), 115-130.
- [14] N. Stanford, M.R. Barnett, *Mater. Sci. Eng. A* 496 (2008) 399–408.
- [15] E.A. Ball, P.B. Prangnell, *Scripta Metall. Mater.* 31 (1994) 111–116.
- [16] S.E. Ion, F.J. Humphreys, S.H. White, *Acta Metall.* 30 (1982) 1909-1919.
- [17] T. Al-Samman, X. Li, *Mater. Sci. Eng. A* 528 (2011) 3809-3822.
- [18] N. Stanford, *Mater. Sci. Eng. A* 565 (2013) 469-475.
- [19] Y. Chino, T. Ueda, Y. Otomatsu, K. Sassa, X. Huang, K. Suzuki, M. Mabuchi, *Mater. Trans.* 52 (2011) 1477-1482.
- [20] S. Ganeshan, S.L. Shang, Y. Wang, Z.-K. Liu, *Acta Mater.* 57 (2009) 3876-3884.
- [21] J. Zhang, Y. Dou, G. Liu, Z. Guo, *Comp. Mater. Sci* 79 (2013) 564-569.
- [22] D.W. Kim, B.C. Suh, M.S. Shim, J.H. Bae, D.H. Kim, N.J. Kim, *Metall. Mater. Trans A* 44 (2013) 2950 – 2961.
- [23] V. Kree, J. Bohlen, D. Letzig, K.U. Kainer, *Pract. Metall.* 41 (2004) 233-246.
- [24] F. Bachmann, R. Hielscher, H. Schaeben, *Solid State Phenomena* 160 (2010) 63-68.
- [25] S.L. Couling, J.F. Pashak, L. Sturkey, *Trans ASM* 51 (1959) 94-107.
- [26] J. Bohlen, S. Yi, D. Letzig, K.U. Kainer, *Mater. Sci. Eng. A* 527 (2010) 7092-7098.
- [27] J. Bohlen, P. Dobron, K. Hantzsche, D. Letzig, F. Chemlik, K.U. Kainer, *Int. J. Mat. Res.* 100 (2009) 790-795.
- [28] P. Dobron, J. Balik, F. Chmelik, K. Illkova, J. Bohlen, D. Letzig, P. Lukac, *J. Alloys Compd.* 588 (2014) 628 – 632.

- [29] J.F. Nie, Y.M. Zhu, J.Z. Liu, X.Y. Fang, *Science* 340 (2013) 957-960.
- [30] J.W. Christian, S. Mahajan, *Prog. Mater. Sci.* 39 (1995) 1–157.
- [31] M.R. Barnett, Z. Keshavarz, A.G. Beer, D. Atwell, *Acta Mater.* 52 (2004) 5093.
- [32] J. Bohlen, P. Dobron, J. Swiostek, D. Letzig, F. Chmelík, P. Lukác, K.U. Kainer, *Mater. Sci. Eng. A* 462 (2007) 302–306.
- [33] R. Cottam, J. Robson, G. Lorimer, B. Davis, *Mater. Sci. Eng. A* 485 (2008) 375–382.

Figure captions

Fig. 1: Microstructure of as-rolled and annealed sheets after varied annealing times; a) ZX10, b) ZXX100 (RD horizontal, ND vertical), c) average grain size of recrystallized microstructures after annealing (60 s to 1800 s)

Fig. 2: Texture of as-rolled and annealed sheets after varied annealing times; a) ZX10, b) ZXX100; (pole figures: RD vertical, TD horizontal, levels: 1.0; 1.5; 2.0; 3.0; 5.0 m.r.d.)

Fig. 3: Boundary map and pole figures of as rolled sections of a) ZX10 and b) ZXX100; black: grain boundary, grey: small angle grain boundary, red: „tensile“ twins, blue: „compression twins“, yellow: double twins (colours in online-version)

Fig. 4: Orientation maps and selected fractions of grains (see text) in the as-rolled and annealed ZX10 and ZXX100 sheets; EBSD-colour scale (in online version): red – (0001), blue {10-10}, green {2-1-10}; colour scale of pole figures same as in Fig. 2.

Fig. 5: Grain fraction analysis of grains with RD tilt or TD tilt orientations as pictured in Fig. 5a for ZX10 a) $GOS < 1^\circ$, b) $GOS > 3^\circ$ and ZXX100 c) $GOS < 1^\circ$, d) $GOS > 3^\circ$.

Figures

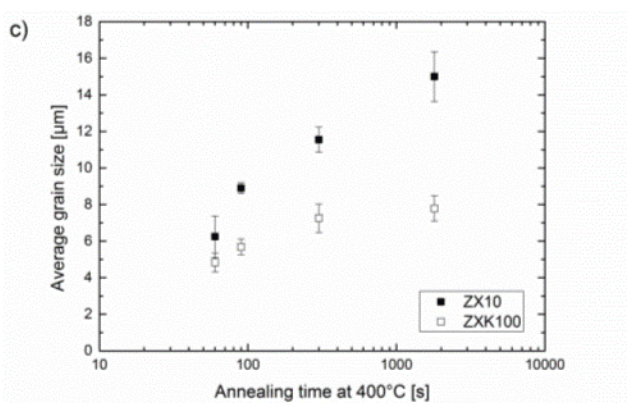
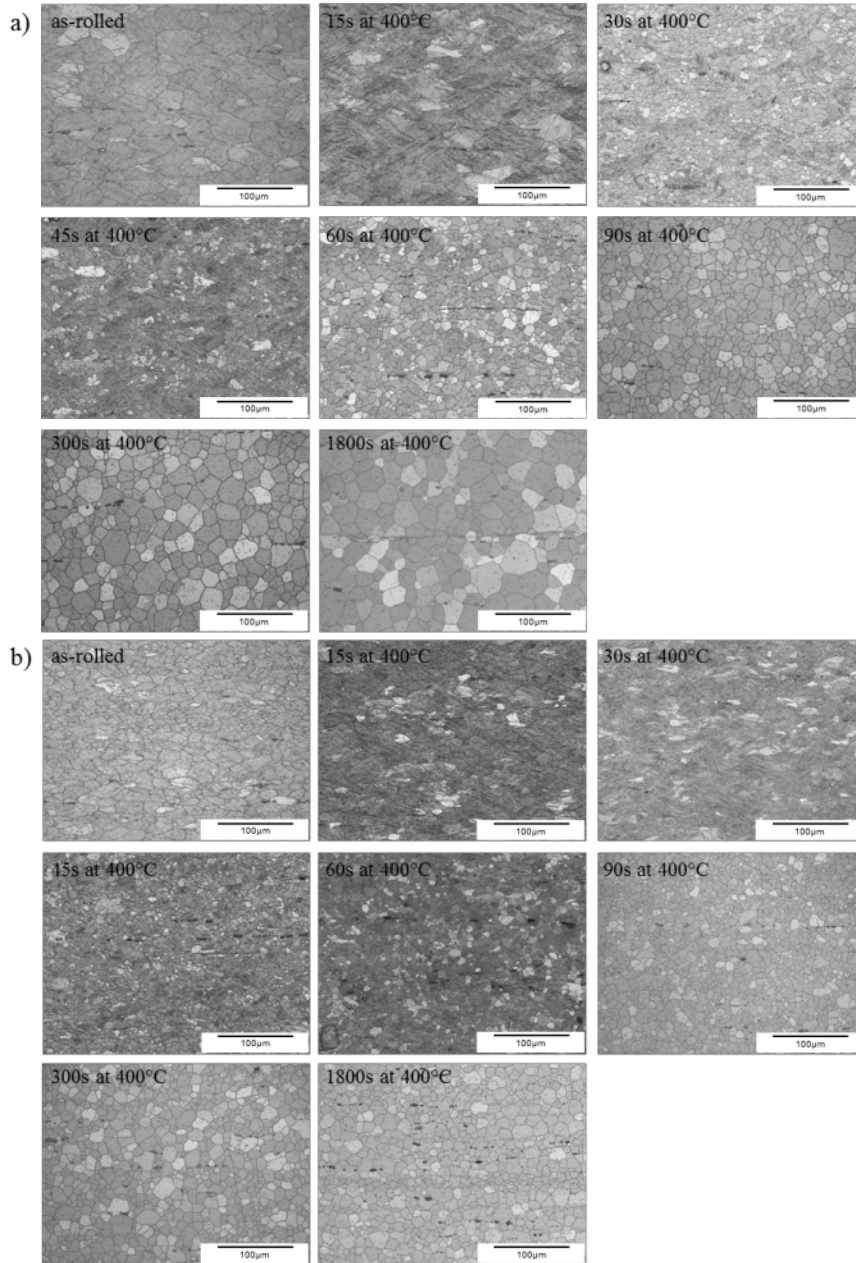


Fig. 1: Microstructure of as-rolled and annealed sheets after varied annealing times; a) ZX10, b) ZXX100 (RD horizontal, ND vertical), c) average grain size of recrystallized microstructures after annealing (60 s to 1800 s)

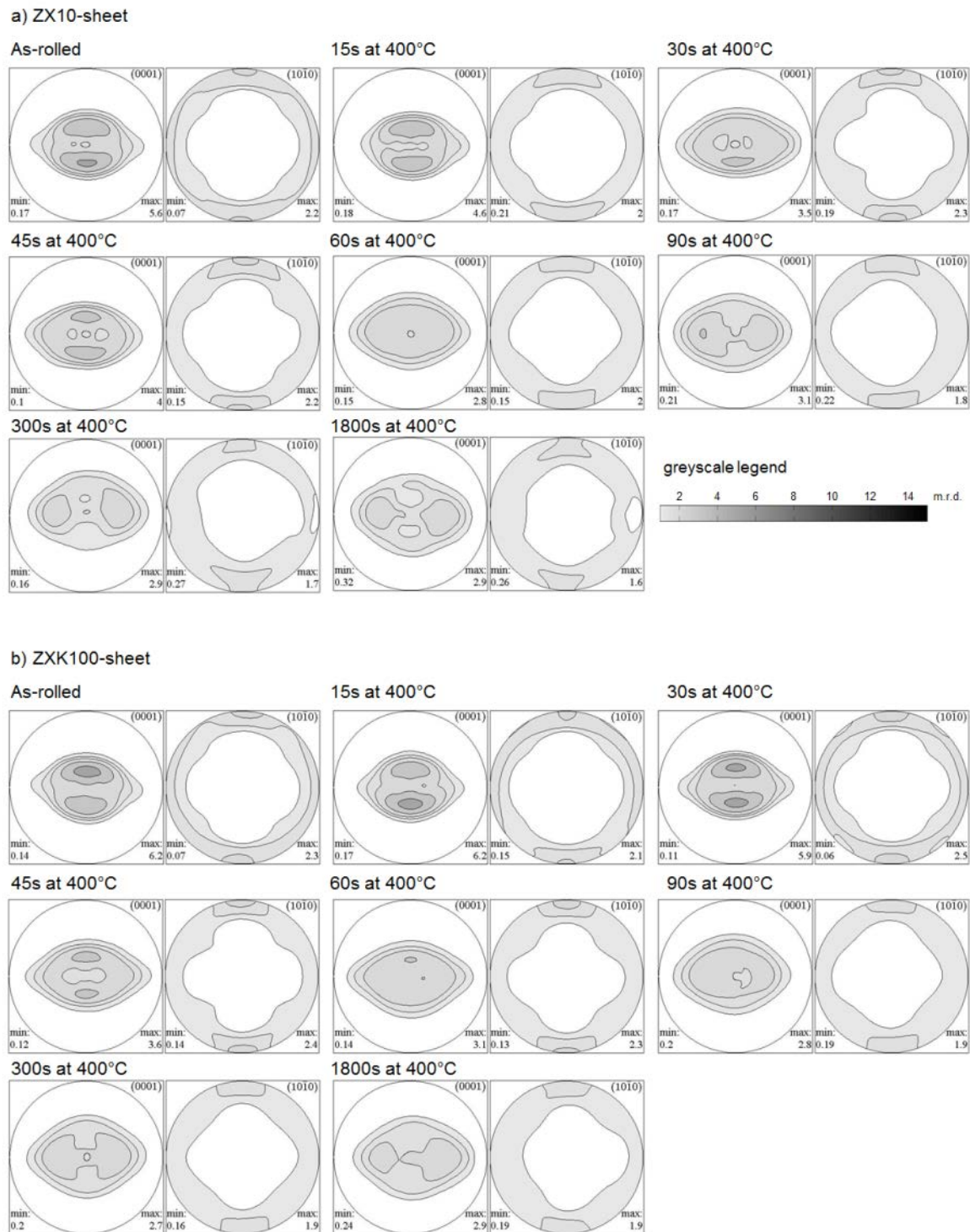
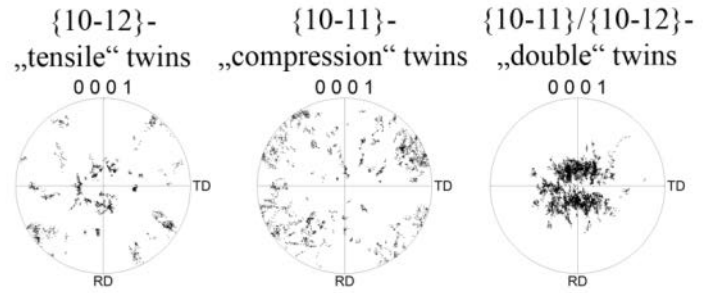
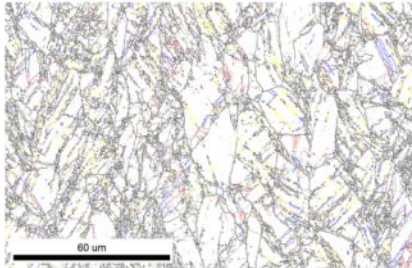


Fig. 2: Texture of as-rolled and annealed sheets after varied annealing times; a) ZX10, b) ZXX100; (pole figures: RD vertical, TD horizontal, levels: 1.0; 1.5; 2.0; 3.0; 5.0 m.r.d.)

a) ZX10



b) ZXK100

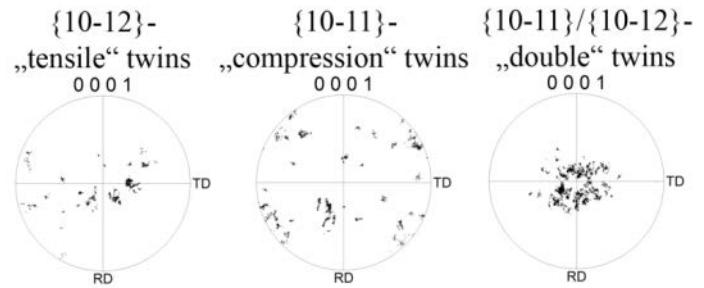
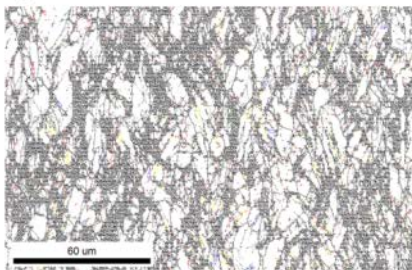


Fig. 3: Boundary map and pole figures of as rolled sections of a) ZX10 and b) ZXK100; black: grain boundary, grey: small angle grain boundary, red: „tensile“ twins, blue: „compression twins“, yellow: double twins (colours in online-version)

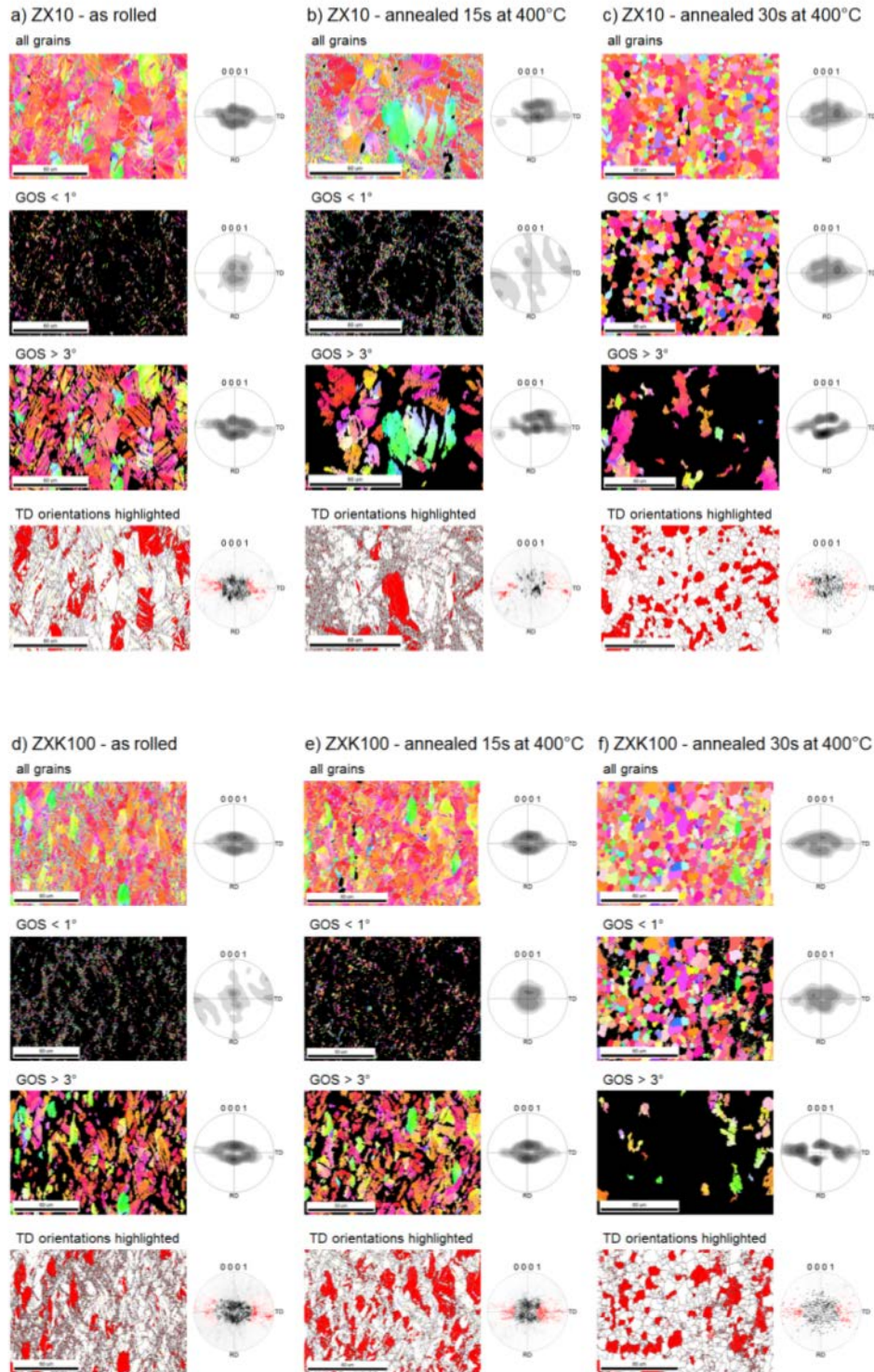


Fig. 4: Orientation maps and selected fractions of grains (see text) in the as-rolled and annealed ZX10 and ZXC100 sheets; EBSD-colour scale (in online version): red – (0001), blue {10-10}, green {2-1-10}; colour scale of pole figures same as in Fig. 2.

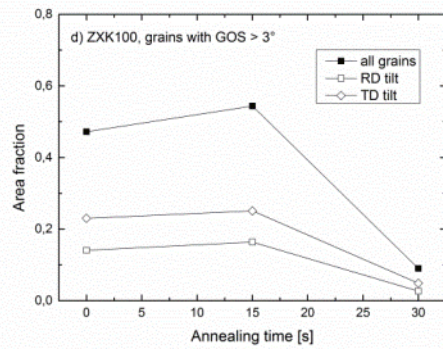
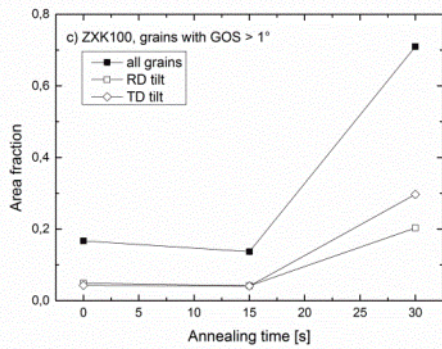
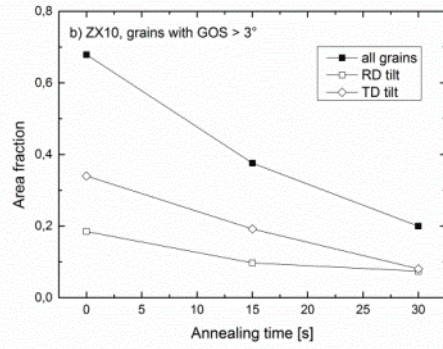
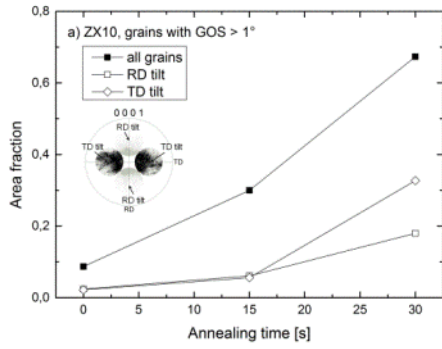


Fig. 5: Grain fraction analysis of grains with RD tilt or TD tilt orientations as pictured in Fig. 5a for ZX10 a) GOS < 1°, b) GOS > 3° and ZXK100 c) GOS < 1°, d) GOS > 3°.